T2R2 東京科学大学 リサーチリポジトリ
Science Tokyo Research Repository

# 論文 / 著書情報
# Article / Book Information

| Citation | Hiroyoshi Tanabe "Fast 3D lithography simulation by convolutional neural network: POC study",Proc. SPIE 11518, Photomask Technology 2020, 115180L,,(2020, 9),doi: https://doi.org/10.1117/12.2575971 |
| --- | --- |
| Copyright notice | Copyright 2020 Society of Photo-Optical Instrumentation Engineers (SPIE). One print or electronic copy may be made for personal use only. Systematic reproduction and distribution, duplication of any material in this paper for a fee or for commercial purposes, or modification of the content of the paper are prohibited. |

Powered by T2R2 (Science Tokyo Research Repository)

PROCEEDINGS OF SPIE

SPIEDigitalLibrary.org/conference-proceedings-of-spie

# Fast 3D lithography simulation by convolutional neural network: POC study

Tanabe, Hiroyoshi, Sato, Shimpei, Takahashi, Atsushi

Hiroyoshi Tanabe, Shimpei Sato, Atsushi Takahashi, "Fast 3D lithography simulation by convolutional neural network: POC study," Proc. SPIE 11518, Photomask Technology 2020, 115180L (20 September 2020); doi: 10.1117/12.2575971

SPIE.

Event: SPIE Photomask Technology + EUV Lithography, 2020, Online Only

Downloaded From: https://www.spiedigitallibrary.org/conference-proceedings-of-spie on 24 Sep 2020 Terms of Use: https://www.spiedigitallibrary.org/terms-of-use

# Fast 3D lithography simulation by convolutional neural network: POC study

Hiroyoshi Tanabe*, Shimpei Sato, Atsushi Takahashi
Tokyo Institute of Technology, 2-12-1 Ookayama, Meguro-ku, Tokyo 152-8550 Japan

## ABSTRACT

Thin mask model has been conventionally used in optical lithography simulation. In this model the diffracted waves from the mask are assumed to be Fourier transform of the mask pattern. This assumption is the basis of Hopkins' method and sum of coherent system model. In EUV (Extreme UltraViolet) lithography thin mask model is not valid because the absorber thickness is comparable to the mask pattern size. Fourier transformation cannot be applied to calculate the diffracted waves from thick masks. Rigorous electromagnetic simulations such as finite-difference time-domain method, rigorous coupled wave analysis and 3D waveguide method are used to calculate the diffracted waves from EUV masks. However, these simulations are highly time consuming. We reduce the calculation time by adapting a convolutional neural network. We construct a convolutional network which can predict the diffracted waves from 1D EUV mask patterns. We extend the TCC method to include the off-axis mask 3D effects. Our model is applicable to arbitrary source shapes and defocus.

**Keywords:** lithography simulation, neural network, EUV mask

## 1. INTRODUCTION

As the semiconductor process node proceeds the mask pattern size becomes close to the absorber thickness. For example, in 20 nm HP (Half Pitch) node, 193 nm immersion lithography is used combined with double pattering process. The mask pattern size is 160 nm HP and the thickness of MoSi absorber is 70 nm. The aspect ratio of the absorber is 0.44. The aspect ratio of the absorber becomes much higher in the case of EUV (Extreme UltraViolet) lithography. In 15 nm HP node the mask pattern size is 60 nm. Typical thickness of Ta absorber is 60 nm and the aspect ratio is 1.

High aspect absorber induces mask 3D effects even in optical lithography.[1] In EUV lithography the situation is more complex due to the oblique incident angle. Well-know EUV specific mask 3D effects are CD (Critical Dimension) difference between horizontal and vertical lines and focus-dependent pattern shift.[2] Another example of the EUV mask 3D effect is the deviation of the phase-shift value near the absorber edges as shown in Fig. 1. Due to the absorber edge effect the optimum phase-shift value of an EUV phase shift mask is largely different from 180 degrees[3]. It is necessary to include the mask 3D effects in EUV lithography simulation.

Rigorous electromagnetic simulation methods such as FDTD (Finite-Difference Time-Domain) method,[4] RCWA[5] (Rigorous Coupled Wave Analysis) and 3D waveguide method[6] accurately calculate the mask 3D effects. However, these simulations are highly time consuming. Semi empirical and fast methods have been developed to include the mask 3D effects approximately in the calculation.[7-10] Recently with the advent of the deep learning software and hardware platforms some attempts have been made to solve the mask 3D effect problems by using deep neural networks.[11-13] The targets of the deep neural networks in these models are the near-field amplitudes calculated by electromagnetic simulations.

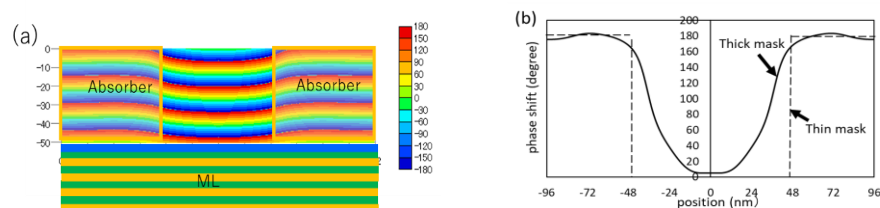


Fig. 1. An example of the mask 3D effect. (a) Reflective wave of an EUV mask and (b) its phase shift value.

*tanabe.h.af@m.titech.ac.jp

Photomask Technology 2020, edited by Moshe E. Preil, Proc. of SPIE Vol. 11518,
115180L · © 2020 SPIE · CCC code: 0277-786X/20/$21 · doi: 10.1117/12.2575971



Downloaded From: https://www.spiedigitallibrary.org/conference-proceedings-of-spie on 24 Sep 2020
Terms of Use: https://www.spiedigitallibrary.org/terms-of-use

Our model also uses a deep neural network to speed up the calculation of mask 3D effects. Here we define the mask 3D effects as the difference between the far-field diffraction amplitudes from a thick mask and those from a thin mask. Since the far-field diffraction amplitudes are described in momentum space, our model can be easily incorporated into TCC (Transmission Cross Coefficient) method[14] and SOCS (Some Of Coherent Systems) model[15] which is conventionally used in optical lithography simulations.

In Sec.2 we explain the difference between the thin mask model and thick mask model. In Sec. 3, as a POC (Proof Of Concept) study, we construct a convolutional neural network which can predict the diffraction amplitudes from 1D EUV mask patterns. In Sec. 4 we extend the TCC method to include the off-axis mask 3D effects.

## 2. THIN MASK MODEL AND THICK MASK MODEL

Figure 2. shows the schematic view of a partial-coherent lithography optics. The light emitted from the secondary source at the position $(s_x, s_y)$ illuminates the mask from the oblique direction $(s_x, s_y)$. The light is diffracted from the mask and it is scattered to the direction $(k_x, k_y)$. The amplitude of the diffracted light from the mask is $U(k_x, k_y; s_x, s_y)$. The diffracted light passes the pupil at the position $(k_x, k_y)$. The pupil cuts the high-frequency components of the diffracted light. Then the diffracted light which passes the pupil forms an image on the wafer.

Total image intensity is the incoherent sum of the image intensities formed by the light emitted from all positions of the secondary source. The total image intensity *I* is calculated by the following formula which is often called as Abbe's theory.

$$I(x,y) = \iint S(s_x, s_y) \left| \iint U(k_x, k_y; s_x, s_y) P(k_x, k_y) e^{-i(k_x x + k_y y)} dk_x dk_y \right|^2 ds_x ds_y \tag{1}$$

where *S* is the source intensity and *P* is the pupil function. The key point of this formula is how to calculate the far-field diffraction amplitude $U(k_x, k_y; s_x, s_y)$.

Thin mask model is conventionally used in optical lithography simulation. The assumption is that the near-field amplitude $U(x, y; s_x, s_y)$ is the product of the incident wave and the mask transmission function $M$ (see Eq. 40 in Sec. 10.6 of Ref. 14).

$$U(x, y; s_x, s_y) = M(x,y) e^{i(s_x x + s_y y)}. \tag{2}$$

As shown in Ref. 14 TCC formula is derived by adapting Hopkins' method with the thin mask model.

In momentum space the far-field diffraction amplitude is written as follows,

$$U(k_x, k_y; s_x, s_y) = \frac{1}{(2\pi)^2} \iint M(x,y) e^{i((s_x - k_x)x + (s_y - k_y)y)} dxdy = M_{\mathrm{FT}}(k_x - s_x, k_y - s_y), \tag{3}$$

where $M_{\mathrm{FT}}$ is the Fourier transform of the mask transmission function. In the thin mask model diffraction amplitude can be calculated easily by Fourier transformation of the mask transmission function.

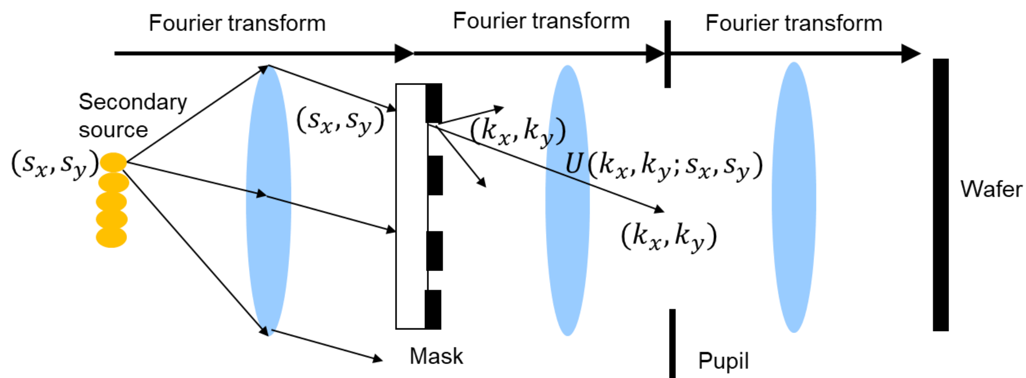


Fig. 2 Schematic view of a partial coherent lithography optics.



Downloaded From: https://www.spiedigitallibrary.org/conference-proceedings-of-spie on 24 Sep 2020
Terms of Use: https://www.spiedigitallibrary.org/terms-of-use

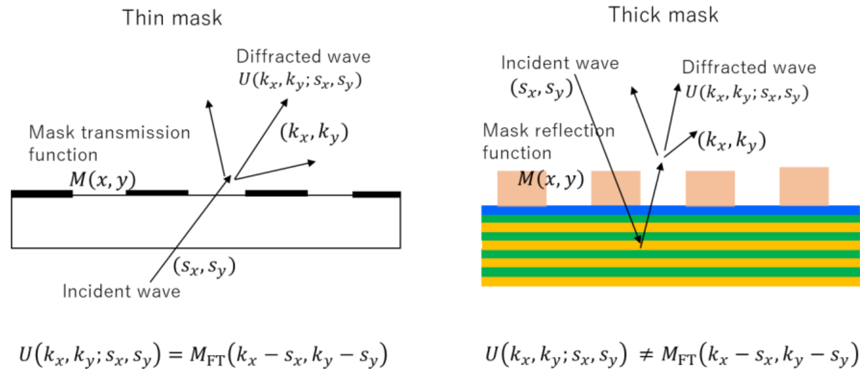


Figure 3. Schematic views of a thin mask and a thick mask.

Equations 2 and 3 are not valid in thick mask model (Fig. 3). Rigorous electromagnetic simulation is required to calculate the diffracted wave accurately. In thick mask model we need to modify TCC formula because we cannot use Eq. 2. We will discuss the details in Sec. 4.

## 3. POC STUDY WITH ONE DIMENSIONAL EUV MASK PATTERNS

In this section we construct a deep neural network which can predict the diffracted wave from a thick mask. We select a CNN (Convolutional Neural Network) which is known to be successful in pattern recognition. In this paper we study one dimensional EUV mask patterns to confirm the feasibility of our model. We also confine the polarization to TE (Transverse Electric) polarization to simplify the problem. For the CNN training targets we perform electromagnetic simulations by using the 2D version[16] of the 3D waveguide mdel.[6]

### 3.1 One dimensional EUV mask pattern with TE polarization

Figure 4 shows a schematic view of a one-dimensional EUV mask pattern. This figure represents a horizontal line pattern as the incident plane is orthogonal to the mask pattern. The electromagnetic wave in free space is decoupled into TE and TM (Transverse Magnetic) polarizations. In one-dimensional case two polarizations will not mix after the diffraction. We select TE polarization where only one electric field $E_y$ remains. Both $E_x$ and $E_z$ are zero for TE polarization. In this way the electric field $E_y$ can be treated like a scalar field $U$ described in the previous section.

The diffracted electric field $E_y$ depends on the incident momentum $s_x$ and outgoing momentum $k_x$. Mask 3D amplitude can be defined as the difference between the thick-mask amplitude $E_y^{\mathrm{EM}}(k_x; s_x)$ (electromagnetic simulation) and the thin-mask amplitude $E_y^{\mathrm{FT}}(k_x - s_x)$ (Fourier transformation).

$$E_y^{\mathrm{EM}}(k_x; s_x) \cong E_y^{FT}(k_x - s_x) + E_y^{\mathrm{3D}}(k_x - s_x) + \partial_{sx} E_y^{\mathrm{3D}}(k_x - s_x) \times (s_x - s_x^{\mathrm{CRA}}). \quad (4)$$

Mask 3D amplitude depends on the incident angle. The dependency impacts on the wafer aerial image when off-axis illumination is used.[10,13] We divide the mask 3D amplitude into two parts, $E_y^{\mathrm{3D}}$ and $\partial_{sx} E_y^{\mathrm{3D}} \times (s_x - s_x^{\mathrm{CRA}})$ . The first part $E_y^{\mathrm{3D}}$ represents the on-axis mask 3D amplitude when the incident angle is at CRA (Chief Ray Angle), 6 degrees and the incident momentum is $s_x^{\mathrm{CRA}}$. The second part $\partial_{sx} E_y^{\mathrm{3D}} \times (s_x - s_x^{\mathrm{CRA}})$ represents the off-axis mask 3D amplitude. We assume here the dependency is linear in $s_x - s_x^{\mathrm{CRA}}$ but we can include higher orders if necessary.

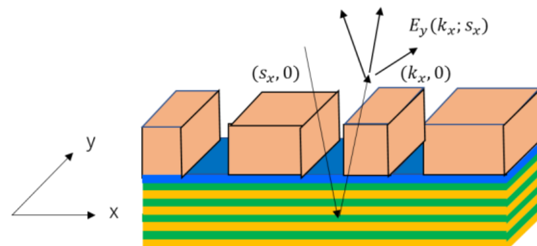


Figure 4. Schematic view of a one-dimensional EUV mask pattern.



Downloaded From: https://www.spiedigitallibrary.org/conference-proceedings-of-spie on 24 Sep 2020
Terms of Use: https://www.spiedigitallibrary.org/terms-of-use

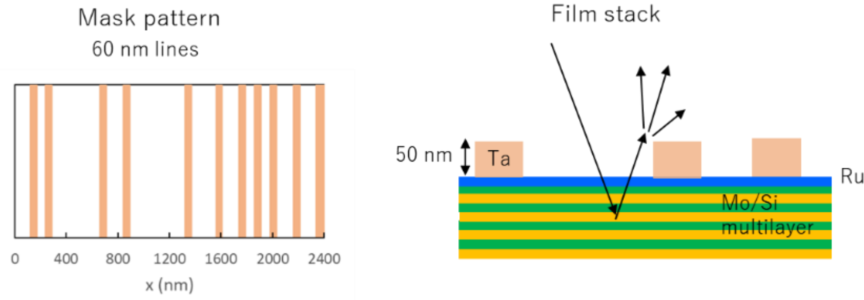


Figure 5. An example of a mask pattern and film stack.

### 3.1 Example of a mask pattern and diffracted waves

Figure 5 shows an example of a mask pattern and its film stack. We assume 60 nm lines on a mask and Ta absorber with 50 nm thickness. A periodic boundary condition with the pitch *L*=2400 nm is used. The diffracted momentum $k_x - s_x$ has discrete values $n \times 2\pi/L$ where *n* is the diffraction order. The largest diffraction order which passes the projection optics is $(1+\sigma)\,NA/4 \times L/\lambda \sim 29$. Here λ is the EUV wavelength 13.5 nm, NA = 0.33 and the maximum σ value is 1. According to Eq. 3 the electric field $E_y$ for each diffraction order *n* is decomposed as follows.

$$E_y^{\mathrm{EM}}(n; s_x) \;\cong\; E_y^{FT}(n) + E_y^{\mathrm{3D}}(n) + \partial_{sx} E_y^{\mathrm{3D}}(n) \times (s_x - s_x^{\mathrm{CRA}}). \tag{5}$$

Figure 6 shows the diffracted waves when the incident wave is at the chief ray angle (on-axis mask 3D effect). The diffracted wave from the thick mask $E_y^{\mathrm{EM}}$ is decomposed into the diffracted wave from the thin mask $E_y^{\mathrm{FT}}$ and the residual mask 3D contribution $E_y^{\mathrm{3D}}$. We can see that the largest amplitude is the 0$^{\mathrm{th}}$ order diffracted wave. The thin mask amplitudes are close to the thick mask amplitudes, but the contribution of the mask 3D amplitudes is non-negligible.

Figure 7 shows the incident angle dependence of the mask 3D amplitudes (off-axis mask 3D effect). The incident angle dependence is not significant. In our model the incident angle dependence of the mask 3D effect is approximated by linear functions of $s_x - s_x^{\mathrm{CRA}}$.

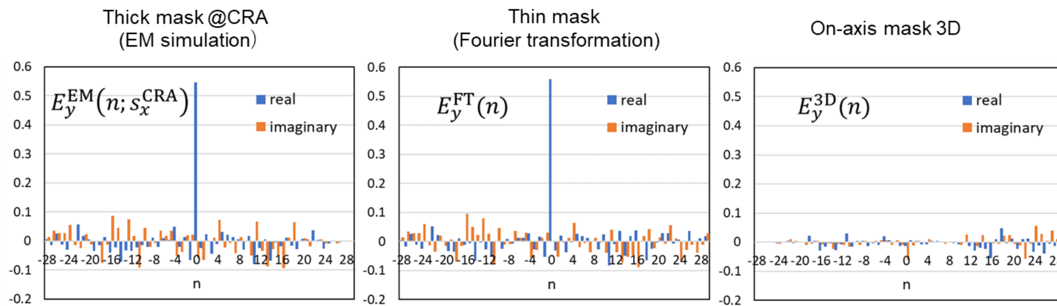


Figure 6. Decomposition of diffracted waves at the chief ray angle.

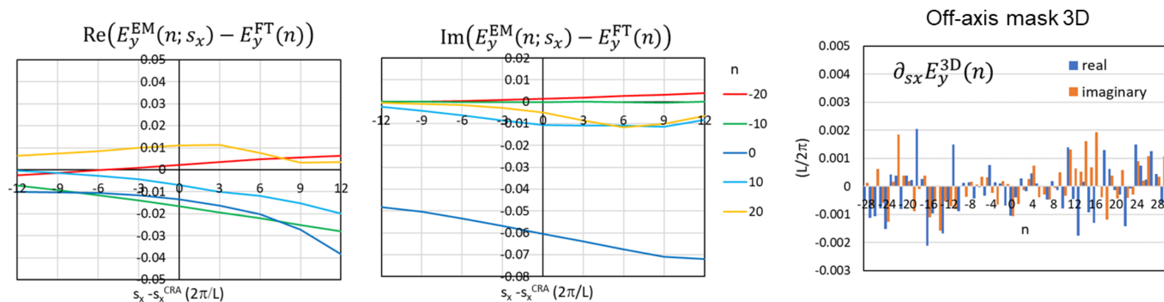


Figure 7. Incident angle dependence of the mask 3D effect.



Downloaded From: https://www.spiedigitallibrary.org/conference-proceedings-of-spie on 24 Sep 2020
Terms of Use: https://www.spiedigitallibrary.org/terms-of-use

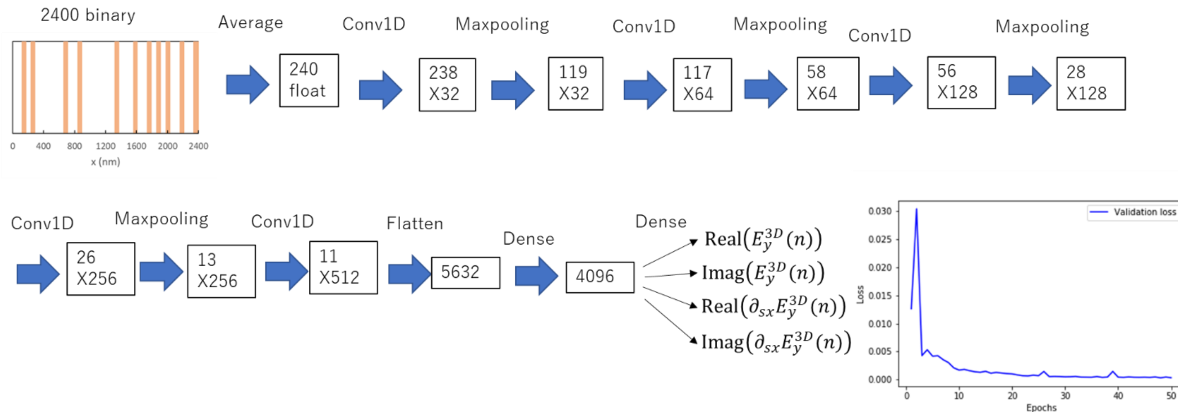


Figure 8. Flowchart of our convolutional neural network.

### 3.2 Convolutional neural network

The diffracted wave from the thin mask $E_y^{\mathrm{FT}}(n)$ is the Fourier transform of the mask reflection function and it can be calculated very fast. Mask 3D effects $E_y^{\mathrm{3D}}(n)$ and $\partial_{sx}E_y^{\mathrm{3D}}(n)$ can be calculated by using electromagnetic simulators but the speed is generally slow. It is obvious that $E_y^{\mathrm{3D}}(n)$ and $\partial_{sx}E_y^{\mathrm{3D}}(n)$ are functions of the input mask pattern. CNNs are conventionally used in pattern recognition. We try to construct a CNN which reproduces the mask 3D effects. We expect that the CNN calculation is much faster than the electromagnetic simulations.

Figure 8 shows the flowchart of our CNN. We use Keras on TensorFlow for the deep learning software. The input mask pattern has 2400 binary data. We first convert them to 240 grayscale numbers by averaging the data. This is the input to the CNN. Inside the CNN we repeat convolutions and maxpoolings several times. Outputs of the CNN are $\mathrm{Real}(E_y^{\mathrm{3D}}(n))$, $\mathrm{Imag}(E_y^{\mathrm{3D}}(n))$, $\mathrm{Real}(\partial_{sx}E_y^{\mathrm{3D}}(n))$ and $\mathrm{Imag}(\partial_{sx}E_y^{\mathrm{3D}}(n))$. In total there is $(2 \times 29 + 1) \times 4 = 236$ targets for CNN.

We generated 99,900 random mask patterns which have 60 nm lines. We calculated the coefficients of mask 3D effects by electromagnetic simulations, and they were the targets of the CNN fitting. The fitting error decreased rapidly during the trainings as shown in Fig. 8.

After the trainings we verified our CNN with 100 new data. Figure 9 shows the results of the verification. The difference between the electromagnetic calculations and CNN is very small. We can successfully predict the mask 3D effects by using the CNN.

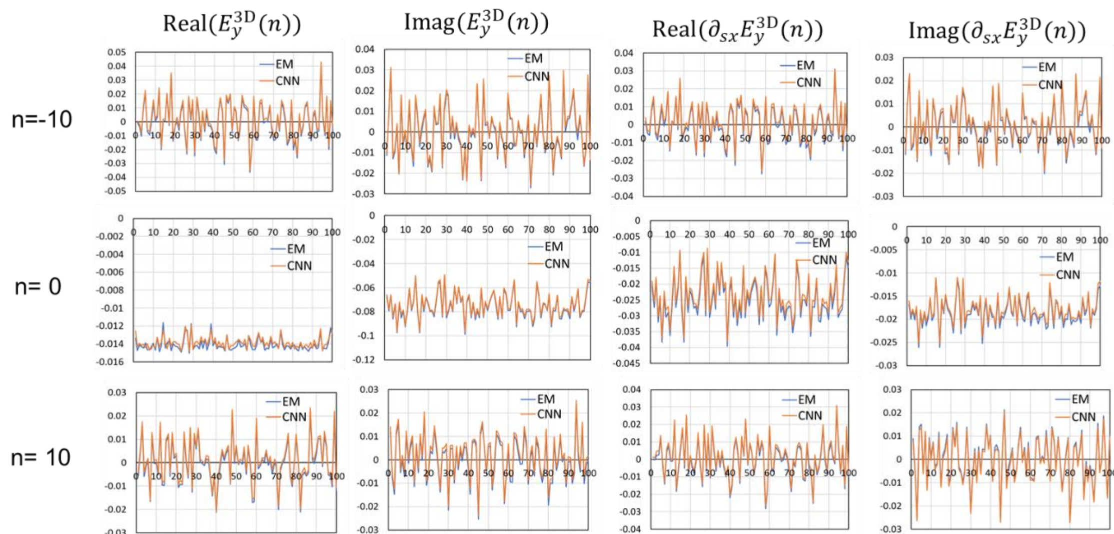


Figure 9. Verification of our convolutional neural networks.



Downloaded From: https://www.spiedigitallibrary.org/conference-proceedings-of-spie on 24 Sep 2020
Terms of Use: https://www.spiedigitallibrary.org/terms-of-use

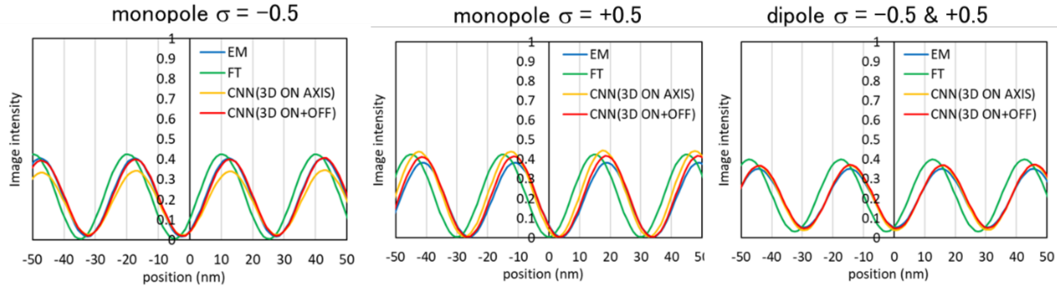


Figure 10. Wafer image intensities of 15 nm L/S.

### 3.3 Image intensity on wafers

We calculate the wafer image intensity of 15 nm L/S by using the diffraction amplitudes predicted by our CNN. Figure 10 shows the results of CNN along with those of the electromagnetic simulation (EM) and the thin mask model (FT).

The calculation time of the electromagnetic simulation is ~500 ms while that of CNN is ~10 ms. We can achieve 50 times speedup by using CNN.

We observe that the peak position of the thin mask model is slightly shifted from that of the electromagnetic calculation. In our lithography simulation we set the mask focus position 92 nm below the absorber surface to compensate the image shift caused by the electromagnetic simulation.[17] The image shift can be interpreted as one of the mask 3D effects of horizontal lines.

The influence of the off-axis mask 3D effect is observed by the difference between CNN (3D ON AXIS) and CNN (3D ON+OFF). It can be clearly seen in the case of the monopole illuminations. However, in the case of the dipole illumination the incident angle dependence is averaged out and the difference is small.

We observe slight difference between EM and CNN (3D ON+OFF) with monopole σ = +0.5 illumination. This could be a CNN error, or a limitation of the linear approximation of the incident angle dependent mask 3D effect.

## 4. EXTENSION OF TCC FOR OFF-AXIS MASK 3D EFFECT

In Sec. 2 we explained that TCC method is not correct for thick mask model. However, we can still use Abbe's theory to calculate the image intensity $I$ of the diffraction amplitude $E_y$ as follows.

$$\begin{aligned} I(x) &= \int S(s_x) \left| \int E_y(k_x; s_x)\, P(k_x) e^{-ik_x x} dk_x \right|^2 ds_x \\ &= \int S(s_x) \left| \int \left( E_y^{\mathrm{FT}}(k_x - s_x) + E_y^{\mathrm{3D}}(k_x - s_x) + \partial_{sx} E_y^{\mathrm{3D}}(k_x - s_x) \times (s_x - s_x^{\mathrm{CRA}}) \right) P(k_x) e^{-ik_x x} dk_x \right|^2 ds_x \\ &= \int S(s_x) \left| \int \left( E_y^{\mathrm{FT}}(k_x) + E_y^{\mathrm{3D}}(k_x) + \partial_{sx} E_y^{\mathrm{3D}}(k_x) \times (s_x - s_x^{\mathrm{CRA}}) \right) P(k_x + s_x) e^{-ik_x x} dk_x \right|^2 ds_x, \end{aligned} \tag{6}$$

By interchanging the order of the integrations, we can get the following formula.

$$\begin{aligned} I(x) \cong & \iint TCC(k_x; k_x') \left( E_y^{\mathrm{FT}}(k_x) + E_y^{\mathrm{3D}}(k_x) \right) \left( E_y^{\mathrm{FT}}(k_x') + E_y^{\mathrm{3D}}(k_x') \right)^* e^{-i(k_x - k_x')x} dk_x dk_x' \\ & + 2\mathrm{Re} \left\{ \iint TCC_x(k_x; k_x') \left( E_y^{\mathrm{FT}}(k_x) + E_y^{\mathrm{3D}}(k_x) \right) \left( \partial_{sx} E_y^{\mathrm{3D}}(k_x') \right)^* e^{-i(k_x - k_x')x} dk_x dk_x' \right\} , \end{aligned} \tag{7}$$

where TCC is the conventional transmission cross coefficient

$$TCC(k_x; k_x') = \int S(s_x)\, P(k_x + s_x) P^*(k_x' + s_x)\, ds_x \tag{8}$$

and $\mathrm{TCC}_x$ is an extended transmission cross coefficient which is required to include the off-axis mask 3D effect.

$$TCC_x(k_x; k_x') = \int (s_x - s_x^{\mathrm{CRA}}) S(s_x)\, P(k_x + s_x) P^*(k_x' + s_x)\, ds_x\,. \tag{9}$$

In Eq. 7 we neglect the term proportional to $\left| E_y^{\mathrm{3D}x} \right|^2$ because the contribution is small.



Downloaded From: https://www.spiedigitallibrary.org/conference-proceedings-of-spie on 24 Sep 2020
Terms of Use: https://www.spiedigitallibrary.org/terms-of-use

Both TCC and $TCC_x$ are Hermitian matrices. Therefore, we can use the eigen value decomposition method in the SOCS model.[15] Our formula can be applied to arbitrary source shapes and defocus. We can accelerate the calculation by selecting small number of the eigen functions which have large eigen values.

# 5. SUMMARY

We have defined the mask 3D amplitude as the difference between the thick-mask and thin-mask diffraction amplitudes. We decomposed the mask 3D amplitude into two parts. One is the on-axis mask 3D amplitude at the chief ray angle, and another is the off-axis mask 3D amplitude which depends on the incident angle of the illumination.

As a POC study we constructed a CNN which can predict the diffraction amplitudes from one dimensional EUV mask patterns. After the training, the CNN successfully reproduced the mask 3D effects. The calculation time was reduced to 1/50 compared to the electromagnetic simulation.

We extended the TCC method to include the off-axis mask 3D effect. Our formula can be applied to arbitrary source shapes and defocus.

As a next step we will try to extend this method to 2D EUV mask patterns by using the 3D waveguide model.[6]

# REFERENCES


[1] J. Finders and T. Hollink, "Mask 3D effects: impact on imaging and placement," Proc. SPIE 7985 (2011)79850I.

[2] A. Erdmann, P. Evanschitzky, G. Bottiglieri, E. Setten and T. Fliervoet, "3D mask effects in high NA EUV imaging," Proc. SPIE 10957 (2019)109570Z.

[3] M.C. Lare, F.J. Timmermans and J. Finders, "Alternative reticles for low-k1 EUV imaging," Proc. SPIE 11147 (2019)111470D.

[4] A. Wong, "TEMPEST users' guide", UCB/ERL M94/64 (1994).

[5] M.G. Moharam and T.K. Gaylord, "Rigorous coupled-wave analysis of planar-grating diffraction," J. Opt. Soc. Am. 71(1981) 811.

[6] K.D. Lucas, H. Tanabe and A.J. Strojwas, "Efficient and rigorous three-dimensional model for optical lithography simulation," J. Opt. Soc. Am. A 13(1996)2187.

[7] K. Adam and A. R. Neureuther, "Simplified modes for edge transitions in rigorous mask modeling," Proc. SPIE 4346 (2001)331.

[8] A. Erdmann, C. Kalus, T. Schmoeller and A. Wolter, "Efficient simulation of light from 3-dimensional EUV-masks using field decomposition techniques," Proc. SPIE 5037 (2003)482.

[9] P. Liu, X. Xie, W. Liu and K. Gronlud, "Fast 3D thick mask model for full-chip EUVL simulations," Proc. SPIE 8679 (2013)86790W.

[10] H. Zhang, Q. Yan, D. Wei and E. Croffie, "A pattern- and optics-independent compact model of mask3D under off-axis illumination with significant efficiency and accuracy improvement," Proc. SPIE 9426 (2015)94260Q.

[11] S. Lan, J. Liu, Y. Wang, K. Zhao and J. Li, "Deep learning assisted fast mask optimization," Proc. SPIE 10587 (2018)105870H.

[12] P. Liu, "Mask synthesis using machine learning software and hardware platforms," Proc. SPIE 11327 (2020)1132707.

[13] R. Pearman, M. Meyer, J. Ungar, H. Yu, L. Pang and A. Fujimura, "Fast all-angle mask 3D ILT patterning," Proc. SPIE 11327 (2020)113270F.

[14] M. Born and E. Wolf, "Principles of Optics," 7th Ed. 1999.

[15] N.B. Cobb, "Fast optical and process proximity correction algorithms for integrated circuit manufacturing," Ph.D. dissertation (University of California, Berkeley, 1998).

[16] C.-M. Yuan, J. Shaw and W. Hopewell, "Modeling of optical alignment images for semiconductor structures," Proc. SPIE 1088 (1989)392.

[17] T. Schmoeller and T. Klimpel, "EUV pattern shift compensation strategies," Proc. SPIE 6921 (2008)69211B.




Downloaded From: https://www.spiedigitallibrary.org/conference-proceedings-of-spie on 24 Sep 2020
Terms of Use: https://www.spiedigitallibrary.org/terms-of-use